SQT

ODS

SIMULATION OF RADIOMETER DATA FROM A SPIN STABILIZED SATELLITE

FINAL REPORT

October 1976

NAS5-22377

S. Rangaswamy

Prepared for

National Aeronautics and Space Administration
Goddard Space Flight Center
Greenbelt Road
Greenbelt, Maryland 20771

OLD DOMINION SYSTEMS INC.
Gaithersburg, Maryland

Unclassified

SECURITY CLASSIFICATION OF THIS PAGE (When Data Entered)

REPORT DOCUMENTATION PAGE		READ INSTRUCTIONS BEFORE COMPLETING FORM
1. REPORT NUMBER NAS5-22377	2. GOVT ACCESSION NO.	3. RECIPIENT'S CATALOG NUMBER
4. TITLE (and Subtitle) SIMULATION OF RADIOMETER DATA FROM A SPIN STABILIZED SATELLITE		5. TYPE OF REPORT & PERIOD COVERED Final - Oct. 1976 6. PERFORMING ORG. REPORT NUMBER
7. AUTHOR(s) S. Rangaswamy		8. CONTRACT OR GRANT NUMBER(s) NAS5-22377
9. PERFORMING ORGANIZATION NAME AND ADDRESS		10. PROGRAM ELEMENT, PROJECT, TASK AREA & WORK UNIT NUMBERS
11. CONTROLLING OFFICE NAME AND ADDRESS Old Dominion Systems, Inc. 4 Professional Drive, Suite 119 Gaithersburg, Maryland 20760		12. REPORT DATE October 1976 13. NUMBER OF PAGES 22
14. MONITORING AGENCY NAME & ADDRESS (if different from Controlling Office)		15. SECURITY CLASS. (of this report) Unclassified 15a. DECLASSIFICATION/DOWNGRADING SCHEDULE
16. DISTRIBUTION STATEMENT (of this Report)		
17. DISTRIBUTION STATEMENT (of the abstract entered in Block 20, if different from Report)		
18. SUPPLEMENTARY NOTES		
19. KEY WORDS (Continue on reverse side if necessary and identify by block number)		
20. ABSTRACT (Continue on reverse side if necessary and identify by block number)		

DD FORM 1 JAN 73 1473 EDITION OF 1 NOV 65 IS OBSOLETE

Unclassified

SECURITY CLASSIFICATION OF THIS PAGE (When Data Entered)

TABLE OF CONTENTS

1.0 Introduction

Satellite infrared (IR) radiometric measurements provide a wealth of data on atmospheric parameters like temperature and humidity profiles. A major problem in this technique is the presence of clouds in the field of view of the radiometer. SMITH et al (1970) have used a statistical method for detecting cloud contamination. The same technique with some modifications is being used as part of an automated set of procedures to produce global maps of sea surface temperature on an operational basis by NOAA. When both IR and visible pictues of the same scene are available, the visible data can be used (SHENK and SOLOMONSON, 1972) to pick out cloudy pixels. A possible problem in this method is the mis-registration of the IR and visible images. Figure 1 shows how such a mis-registration can show that a visible pixel is clear while the corresponding IR pixel is cloudy.

In the present study the effect of mis-registration on cloud brightness threshold is investigated by simulating radiometric data as observed from a spin stablized synchronous satellite such as the SMS. Clouds are introduced randomly and a bi-directional reflectance model is used to create radiance data from clouds and ocean. As part of this study a theoretical and an empirical reflectance model are compared.

2.0 Brightness Normalization

2.1 Introduction

Brightness normalization is the technique of adjustment of visible radiance data measured under different illumination and viewing conditions (Figure 2) to a standard configuration of

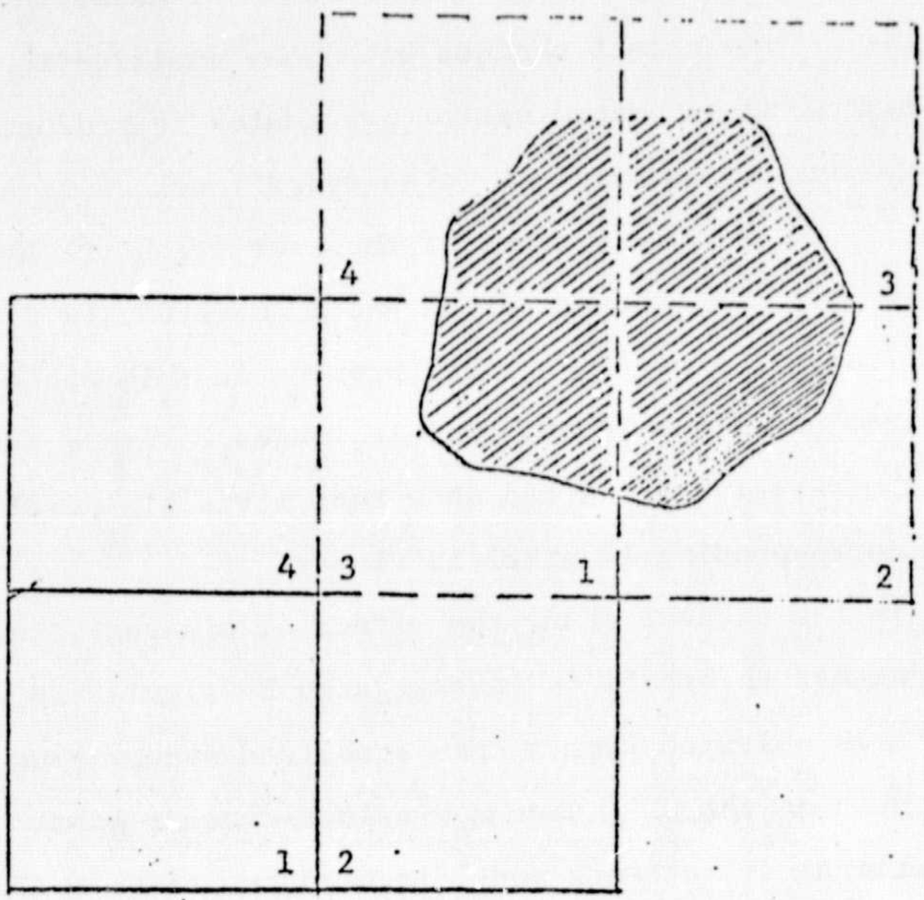

FIGURE 1

Registration offset between visible (continuous lines) and IR (dashed lines). Irregular contour represents cloud.

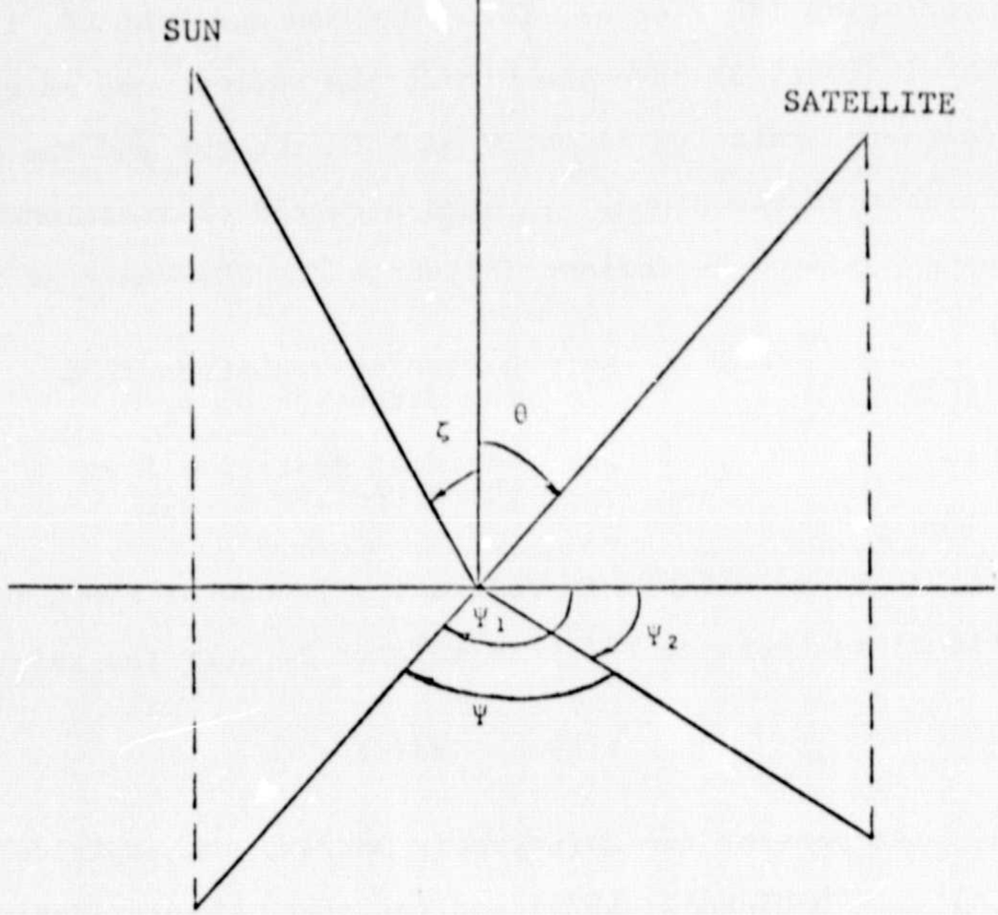

Figure 2 Geometry of Reflection

solar illumination and sensor viewing. This is necessary in applications where intercomparison of cloud albedo has to be made. The simplest normalization procedure would be to assume that clouds are perfectly diffuse reflectors which obey Lambert's law. However, studies of the angular distribution of reflected solar radiation (RUFF et al, 1970, BRENNAN and BANDEEN, 1970, RASCHKE et al, 1973) have shown that the reflectance of clouds depends on the relative geometry of both the sun and the satellite with respect to the cloud. In such a case a bidirectional reflectance ρ has to be defined (SIKULA and VONDERHAAR) as follows:

$$\rho(\xi, \theta, \psi) = \frac{\text{Reflected radiation from the direction } \theta, \psi_2}{\text{Incident radiation from the direction } \xi, \psi_1} \tag{1}$$

where ξ, θ, ψ are defined in Figure 1. It can be shown that the directional reflectance r (ξ) is related to ρ by the relation

$$r(\xi) = \pi\rho(\xi) \tag{2}$$

At present two anisotropic models, one empirical (SIKULA) and VONDERHAAR, 1972) and the other theoretical (MOSHER, 1974) are available for normalizing cloud brightness.

2.2 Empirical Model

SIKULA and VONDERHAAR (1972) have synthesized an empirical bidirectional model by using observations of cloud reflectances by BRENNAN and BANDEEN (1970) as well as available summaries presented by RASCHKE et al (1971). Figure 3 shows a vertical cross-section of the model.

The empirical model has the following defects:

a. It has a restricted data base in the sense that reduction of variance in reflectance will require a much larger number of observations than have been actually used.

b. For purposes of cloud height estimation the optical thickness will not be available as a parameter of the model.

It also has the following advantages:

a. It is simple to use.

b. It can be updated continually, as and when new observations become available.

c. Its empirical nature frees it from errors due to assumptions inherent in the theoretical model. In other words, it is 'true to life'.

2.3 Theoretical Model

The light reflected from a cloud depends on the following variables (MOSHER, 1974):

a. Shape and size distribution of particles.

b. Number density of scattering particles.

c. Cloud thickness

d. Angular configuration of sun, cloud, and satellite

e. Shape of the cloud

MOSHER (1974) has developed a model of cloud reflectances by theoretically calculating the multiple scattering of light in a cloud for a range of optical thicknesses of the cloud. The multiple scattering program is the one developed by HANSEN (1971). MOSHER (1974) has computed the intensity of reflected light from the cloud for a range of elevation angles of the sun and the satellite as well as the relative azimuth angle between them. The model is thus four dimensional. Three angles and the optical thickness of the cloud are the parameters of the model. Given the satellite-cloud-sun geometry and the measured radiance, it will then be possible to pick out the optical thickness from the model.

The theoretical model has the following defects:

a. The theoretical model neglects both Rayleigh scattering and molecular absorption. At small optical thicknesses, the former may have to be taken into account. There is a possibility (CURRAN, 1975) that absorption due to ozone may be large enough to be taken into account.

b. The multiple scattering computation using the doubling method cannot take the finite horizontal dimension of the cloud into account. There is evidence from Monte Carlo calculations (MCKEE and COX, 1974, DAVIES, 1975, MCKEE and COX, 1975) that there is a considerable leak of radiation through the sides of the cloud. The theoretical model corrects for this effect by an arbitrary adjustment of a scaling factor used to convert input digital counts into radiance data. The factor was adjusted to give 'reasonable results' when the emissivity of cirrus clouds was computed.

c. Finally, the method of computing percentage cloud cover is open to question. However, the vexing problem of partial cloud cover in a resolution element is one which is common to all satellite radiometric data.

The model has the following advantages:

a. It is also simple to use.

b. It yields optical thickness as an extra parameter which makes it more suitable for cloud height estimation.

2.4 Conclusions

The theoretical approach becomes 'empirical' when the calibration factor is adjusted. The validity of such an adjustment has to be tested by calibrating the visible data independently. A good check on the MOSHER model would be a comparison with results obtained from Monte Carlo calculations for the same angular configuration for finite clouds. The calibration factor for very thick convective clouds of finite horizontal dimensions can then be computed from the Monte Carlo results.

When these checks show the theoretical model to be a valid one, it will be obviously superior to the empirical model.

3.0 Simulation of Visible Radiances as Observed from a Synchronous Satellite

Simulation of radiance data involves the following procedures:

1. The starting and ending numbers of lines and pixels of the grid under consideration are assumed. The dimensions of the grid were taken to be 64 by 64.
2. In the case of a spin stabalized synchronous satellite like the SMS the mapping raster is formed by a combination of satellite spin motion and a step action of the scanner optics. Assuming the orbit and attitude parameters of satellite, to be the nominal values of SMS-1, the rotation matrix for conversion from the satellite coordinates (Figure 4) to earth-fixed coordinates (Figure 5) is computed.
3. For each pixel the pointing vector from the spacecraft to the pixel is computed in satellite coordinates, and then transformed to earth-fixed coordinates through the rotation matrix. The piercepoint of this vector with the earth ellipsoid is then computed. The latitude and longitude of each pixel are then easily obtained.
4. Cloud cover was simulated by assuming that one quarter of the 64 x 64 pixels had clouds with randomly varying areas in them. Uniformly distributed random numbers varying in magnitude from 0 to 1 were generated for this purpose.
5. The bidirectional reflectance pattern of SIKULA and VONDERHAAR (1972) was used to compute the albedo A

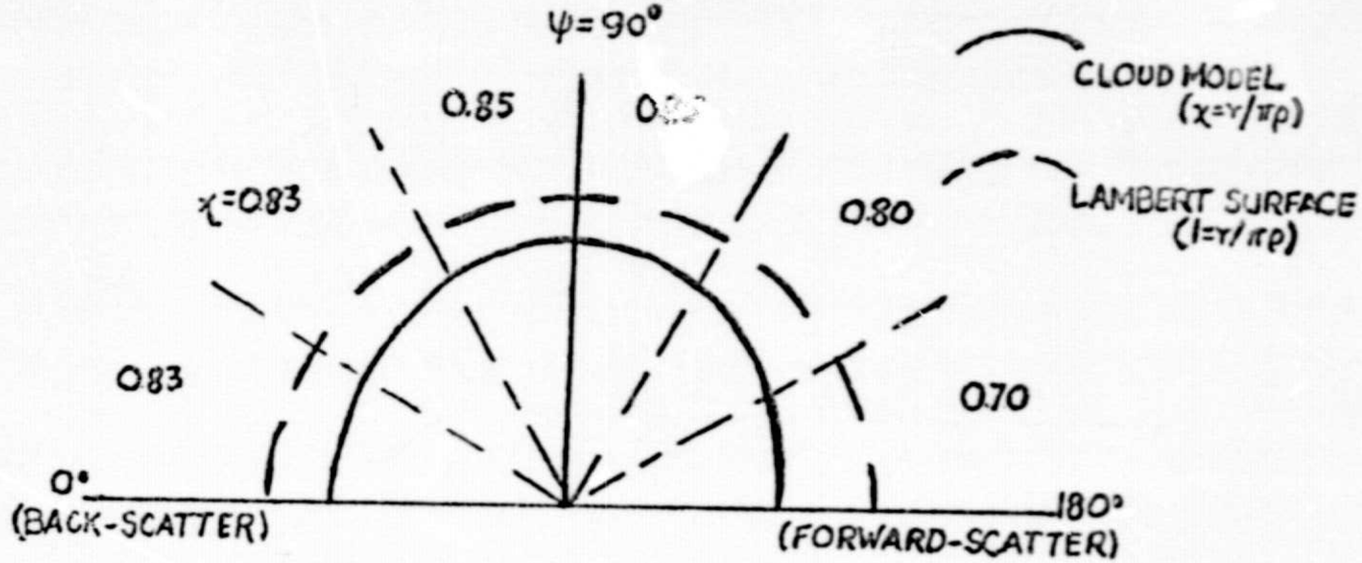

FIGURE 3

Vertical cross-section through the χ model for a cloud, showing the Lambert reflectance and that of actual clouds.

$\xi = 35^{o}\text{-}60^{o}$ $\theta = 40^{o}\text{-}50^{o}$ $\psi = 0\text{-}180^{o}$

(After SIKULA and VONDERHAAR, 1972)

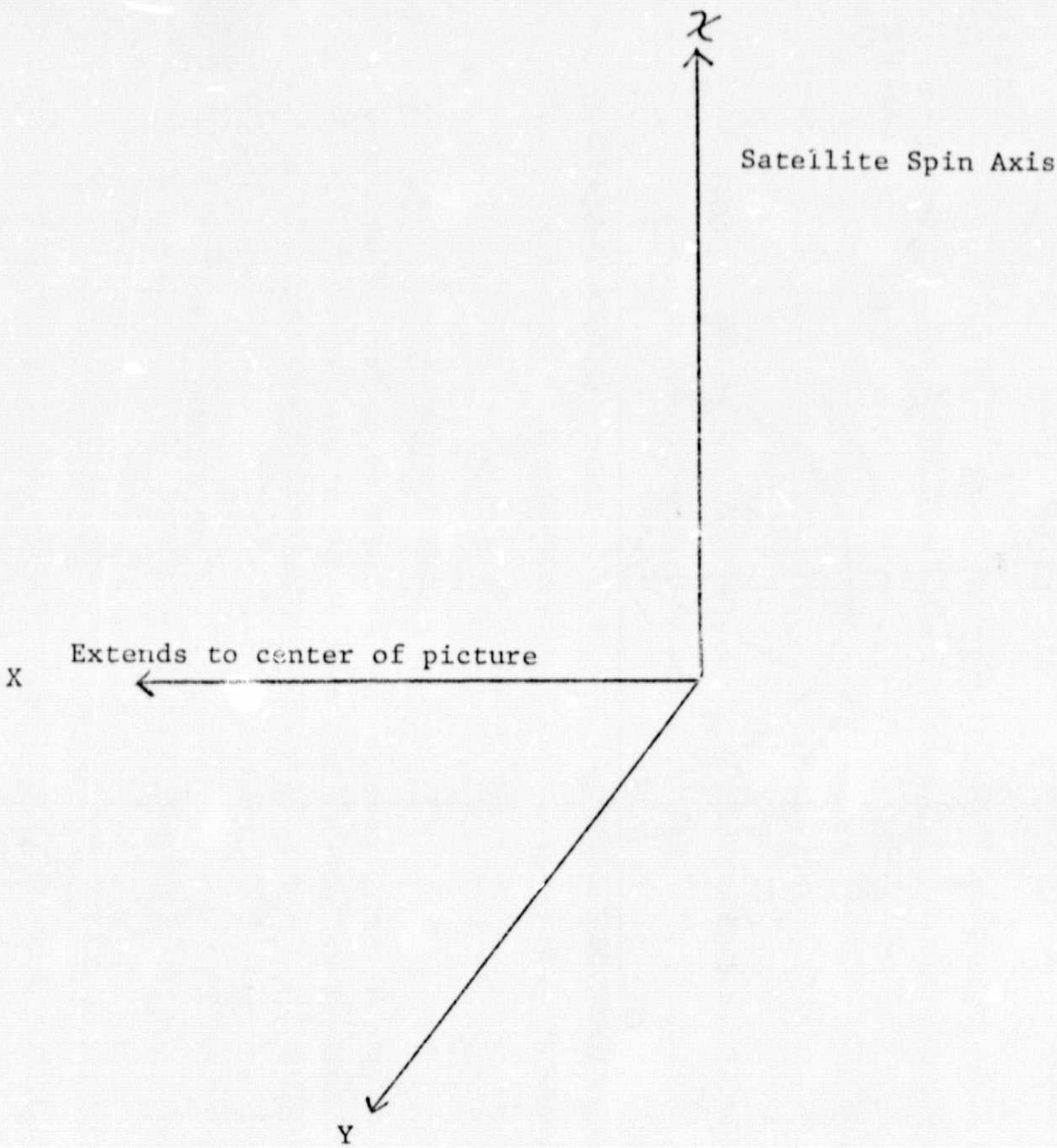

FIGURE 4

Satellite Coordinate System

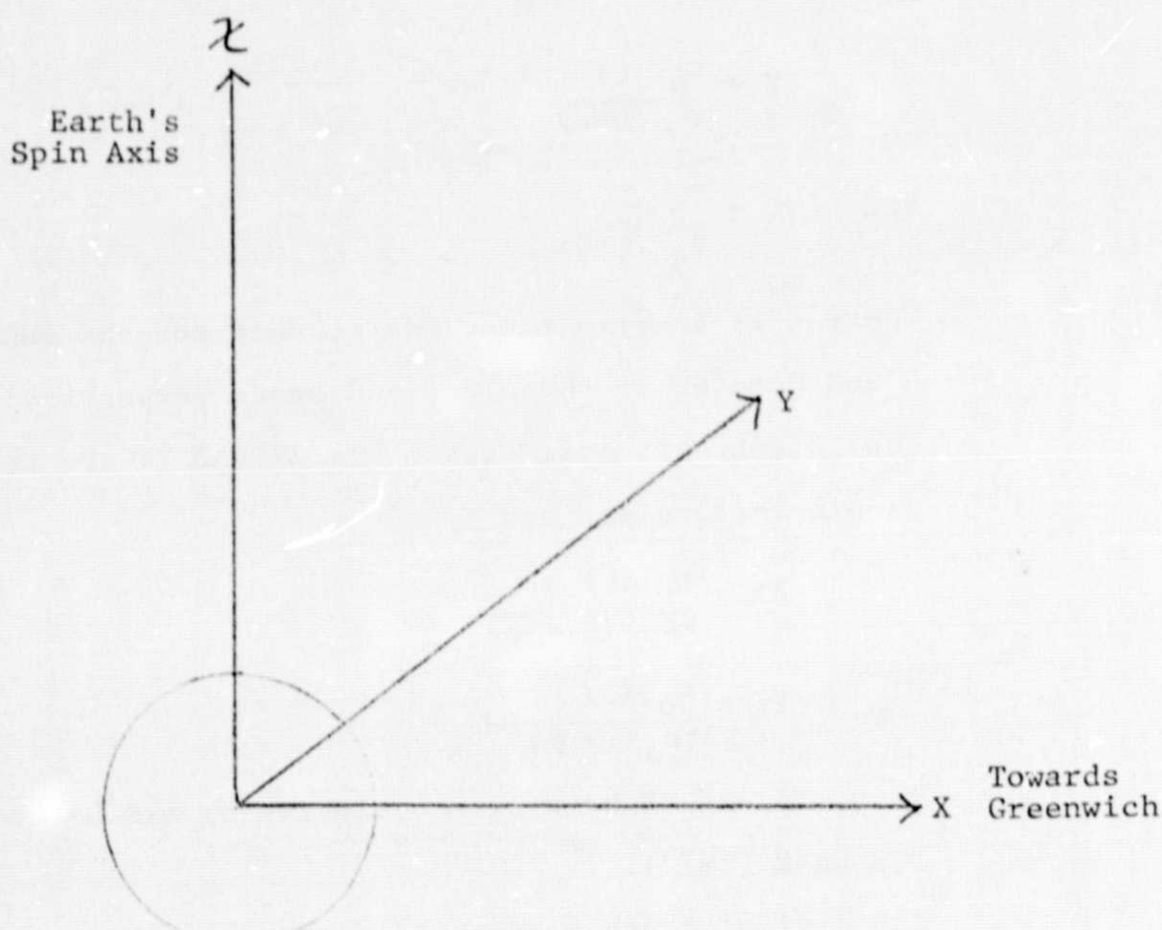

FIGURE 5

Earth Fixed Coordinates

observed by the satellite where A is given by

$$A = \left(\frac{0.03.P.C.}{XX} + \frac{0.7.Q.(1-C)}{YY}\right) \cos\xi \qquad (3)$$

The numbers .03 and .7 refer to the zenith albedo of the ocean and clouds respectively. P and Q are defined by

$$P = \frac{r_o\ (\xi)}{r_o\ (\xi=0)} \qquad (4)$$

and $$Q = \frac{r_c\ (\xi)}{r_c\ (\xi=0)} \qquad (5)$$

Where r is the isotropic reflectance and the subscripts C and O refer to the cloud and ocean respectively. P is the anisotropic reflectance and XX and YY are the anisotropic factors defined by

$$XX = \frac{r_c\ (\xi)}{\pi\rho_c\ (\xi,\Theta,\psi)} \qquad (6)$$

$$YY = \frac{r_o\ (\xi)}{\pi\rho_o\ (\xi\Theta,\psi)} \qquad (7)$$

P, Q, XX and YY have been tablurated by SIKULA and VON DER HAAR (1972).

The digital count corresponding to the albedo sensed by the radiometer was taken as D where

$$D = 62.8\sqrt{A} \qquad (8)$$

which is the nominal calibration function for the VISSR instrument (BRISTOR, 1975). Observational noise was added to the digital counts by generating Gaussian random numbers with a standard deviation of 1 count. A sample of the simulated digital counts over a clear ocean area can be seen in Figure 6.

FIGURE 6

DIGITAL COUNTS OF VISIBLE RADIANCE

8	8	9	9	8	9	8	8	8	8	8
9	9	9	8	8	8	8	9	8	8	8
8	9	8	8	8	8	9	9	8	9	8
8	9	9	10	9	8	8	9	8	10	8
9	9	8	8	8	9	9	8	8	9	9
9	9	8	7	9	8	9	8	8	8	9
8	8	8	8	8	8	8	8	8	8	9
9	8	8	9	8	9	8	9	8	9	9
8	7	9	8	8	8	8	8	9	8	9
9	8	9	9	9	8	9	9	8	8	8
9	7	9	8	8	8	8	8	9	8	7

4.0 Determination of Visible Brightness Threshold for Clouds

The digital counts of albedo over the 64 x 64 grid are normalized by dividing by $\cos\xi$, under the assumption of isotropic reflectance. This is because the anisotropic reflectance for ocean is different from that for clouds. Unless the percentage cloudiness of a pixel is known, it is not possible to use the anisotropic reflectance model for normalization. A histogram of the normalized reflectance was then created. Figure 7 shows a computer plot of the histogram. The horizontal scale shows both the sequential interval class and the normalized reflectance corresponding to the interval. Interval 1 contains values less than 8 and interval 20 all valves exceeding 20. The occurrence frequency in each interval is given in the top line. From Figure 8 it may be seen that the histogram is asymmetric. The peak in the histogram corresponds to the predominant clear ocean area. Points to the left of the peak are due to the assumed observational noise. SHENK and SALOMONSON (1972) determined the width of the despersion Δr due to noise on ocean reflectances from the histogram. The brightness threshold was then set as $r_p+\Delta r$ where r_p is the modal value of reflectance.

FIGURE 7

HISTOGRAM OF NORMALIZED REFLECTANCES $\xi = 19.6$ $\Theta = 58.4$ $\psi = 60.6$

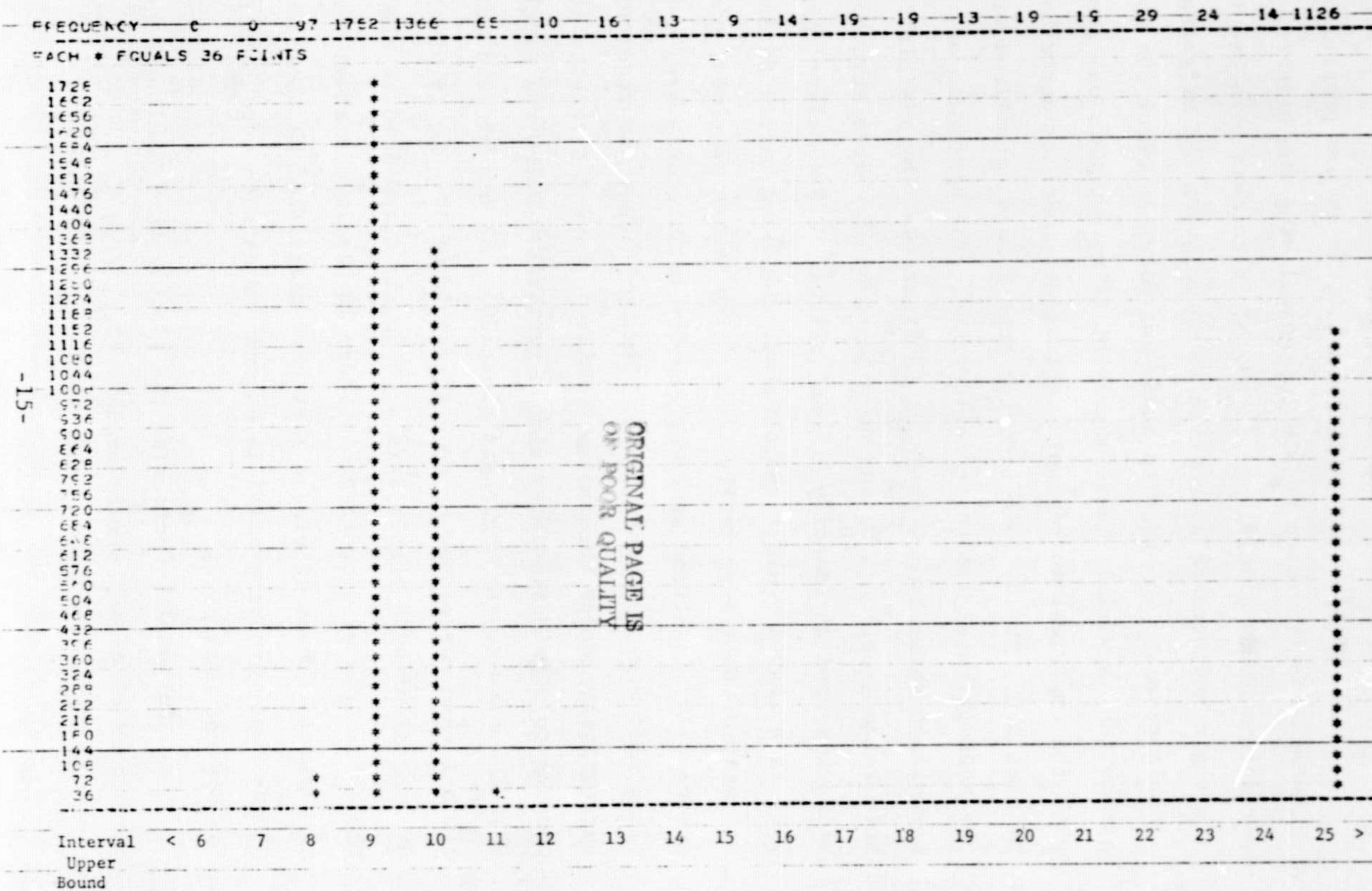

5.0 Error due to Isotropic Normalization

As pointed out in Section 4.0, it is not possible to use anisotropic reflectance models for normalizing the brightness of partially cloudy pixels. It is therefore necessary to use the isotropic reflectance assumption in normalizing the brightness of visible pixels. In order to study the possible error due to this assumption, a visible image matrix of 64 x 64 pixels was generated with the empirical anisotropic reflectance model as described in Section 3.0. The visible radiance counts were normalized with the assumption of isotropic reflectance. The histogram of normalized reflectances is shown in Figure 7. The visible threshold value (Section 4.0) can be seen to be 11. This threshold value was used to identify 'clear' pixels. These 'clear' pixels were then tested against the original simulated matrix to determine how many of them were really clear. The number of cloudy pixels erroneously classified as clear and the total cloudy area wrongly classified were thus identified. This procedure was repeated for successively larger thresholds. Table I shows the results corresponding to a grid simulated almost vertically below the satellite when the sun's zenith angle was about 20^{o}. It can be seen from Table I that corresponding to a threshold of 11 only 16 pixels out of a total of 4096 pixels were erroneously classified as cloudy. The total area of cloudiness in these 16 pixels was about a seventh of a pixel. These 16 pixels that were classified as clear contained clouds that were very small in extent and as such were comparable to observational noise.

Obviously, increasing the visible threshold will increase the number of cloudy pixels wrongly classified as clear. However, for a random cloud model the visible threshold can be increased beyond the $r_p + \Delta r$ value (Section 4.0) without incurring serious error on a statistical basis. From Table I it can be seen that increasing the threshold from 11 to 18 will increase the total cloudy area wrongly classified as clear to 4 pixels out of a total of 4096 pixels.

TABLE I

$\xi = 19.6$ $\Theta = 58.4$ $\Psi = 60.6$

Visible Threshold (Normalized Radiance Counts)	Number of Cloudy Pixels Erroneously Classified as Clear	Total Area Classified Erroneously as Clear (Units of Pixels)
11	16	.14
12	22	.29
13	35	.72
14	45	1.19
15	53	1.57
16	61	2.02
17	73	2.90
18	86	3.96
19	94	4.72
20	107	6.11

However, if there was a very thin layer of cloud which increased the brightness by say 7 counts, the error in the surface temperature estimation due to the relaxed threshold will be considerable.

To investigate the effect of the geometric configuration of satellite and sun with respect to the area under consideration, a 64 x 64 matrix was generated nearer the limb, were the values of ξ, Θ and ψ differed considerably from the previous case. The histogram of normalized reflectances for this case is shown in Figure 8. The visible brightness threshold in this case can be seen to be 18. The number of cloudy pixels erroneously classified as clear corresponding to various thresholds is shown in Table II.

FIGURE 8

HISTOGRAM OF NORMALIZED REFLECTANCES $\xi = 58.9$ $\theta = 48.9$ $\psi = 8.3$

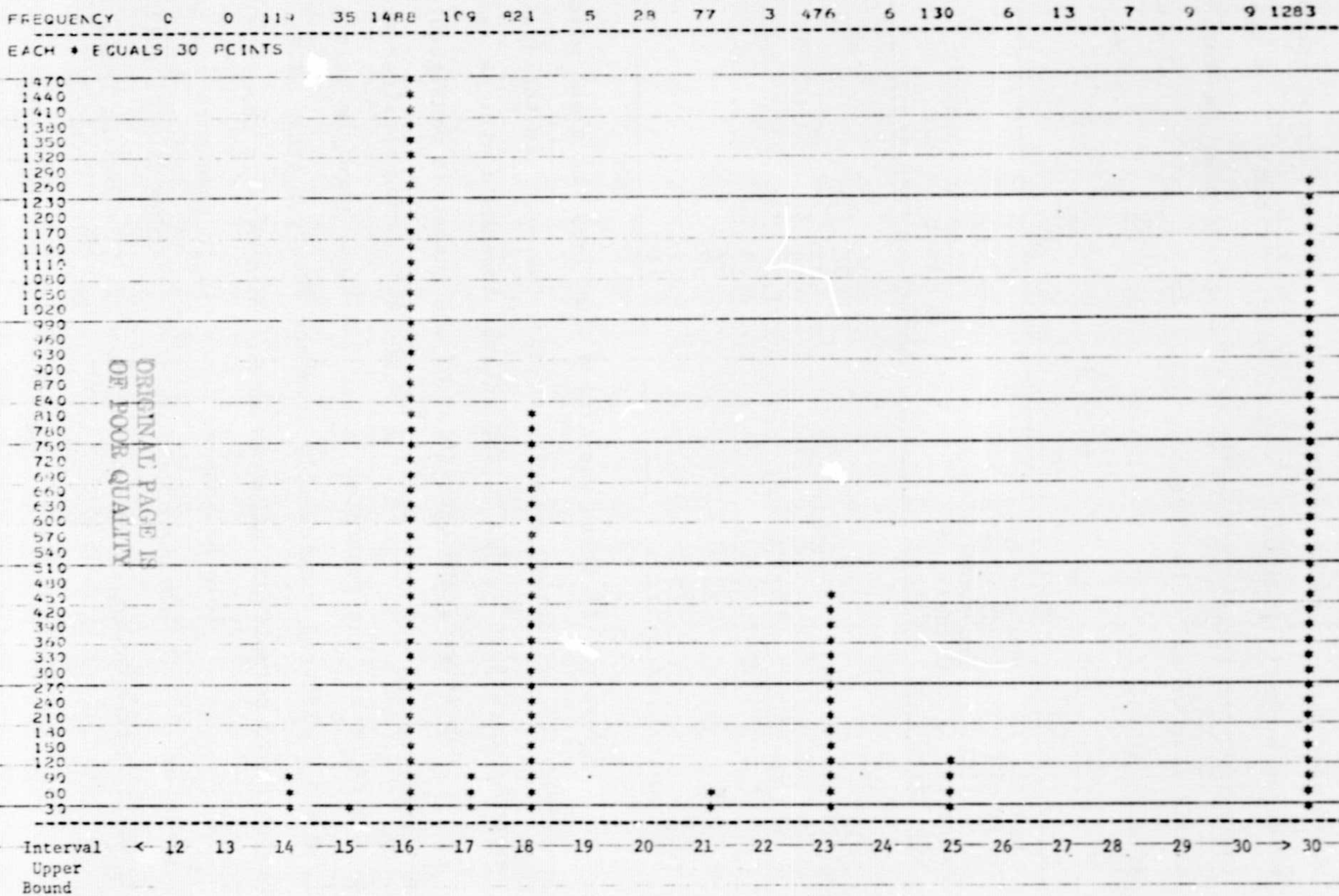

In this case also the error due to relaxation of the threshold can be seen to be small. Although the isotropic normalization will lead to different values of the threshold for different geometric configurations of sun and satellite, the use of the brightness threshold value does not introduce significant error. This is because the brightness threshold selection technique is a statistical one and error due to isotropic normalization acts like a constant bias over small areas.

TABLE II

$\xi = 58.9$	$\theta = 48.9$	$\Psi = 8.3$
Visible Threshold (Normalized Radiance Counts)	Number of Pixels Erroneously Classified as Clear	Total Area Erroneously Classified as Clear (Units of Pixels)
18	8	.06
19	8	.06
20	12	.12
21	12	.12
22	14	.18
23	21	.31
24	27	.55
25	35	.89
26	39	1.10
27	47	1.41

6.0 Effects of Spatial Misregistration Between Visible and IR Data.

In order to use the brightness threshold of clouds obtained from the visible data to identify clear column IR pixels, it is necessary for the IR and visible pixels matrices to be in exact spatial alignment. If the IR and visible images are misaligned then the identification of clear column IR pixels from the visible data leads to error.

The effect of misregistration on the cloud filtering process was tested by creating a visible radiance matrix of dimensions 64 x 64 pixels with a constant offset along each line from the IR matrix. In other words, the simulated misregistration between the IR and visible matrices was only along the lines and none across them. Such a misregistration has been observed the SMS VISSR data.

For a given offset the number of cloudy pixels wrongly classified as clear was determined for different visible thresholds. Table III gives the results for an offset of one pixel along each line. It may be seen from Table III that there is a sharp increase in the area wrongly classified as clear. The error is clearly unacceptable. To illustrate this effect further, the offset between the IR and visible matrices was increased to 4 pixels along the line only. The errors resulting from this can be seen in Table IV. It is obvious from Table IV that the increase in registration offset increases the error enormously.

TABLE III

Visible Threshold (Normalized Radiance Count)	Number of Clouds Erroneously Classified as Clear	Total Area Erroneously Classified as Clear (In Units of Pixels)
11	72	41.2
12	78	44.3
13	90	49.2
14	99	54.5
15	105	58.2
16	113	61.8
17	124	67.0
18	136	73.1

It has to be remembered that the above results refer to a cloud model that is random. In real data cloud strata are clearly identifiable and only scattered clouds within the field of view cannot be visually identified. A random cloud model can represent one realization of such scattered clouds within the field of view. The results shown in Table III and IV are valid for such cases.

TABLE IV

Visible Threshold (Normalized Radiance Count)	Number of Clouds Erroneously Classified as Clear	Total Area Erroneously Classified as Clear
11	239	125.5
12	245	129.2
13	256	133.7
14	264	140.1
15	269	143.6
16	277	147.0
17	287	151.1
18	295	154.3

The conclusion to be drawn from these results is that the IR and visible data have to be spatially registered to an accuracy of at least one pixel for the purpose of cloud filtering of IR data by using a visible brightness threshold.

REFERENCES

1. Brennan, B. and W. R. Bandeen, 1970, Journal of Applied Optics, Volume 9, Number 2.

2. Bristor, C. L., 1975, NOAA Tech. Memo NESS-64.

3. Curran, R., Personal Communication, 1975.

4. Davies, R., Collection of Abstracts of the Second Conference on Atmospheric Radiation, October 29-31, 1975, Arlington, Virginia.

5. Hansen, J.E., Journal of Atmospheric Sciences, 28, 1400-1426, 1971.

6. McKee, T. and S. K. Cox, Journal of Atmospheric Sciences, 31, 1885-1892, 1974.

7. McKee, T. and S. K. Cox, Collection of Abstracts of the Second Conference on Atmospheric Radiation, October 29-31, 1975, Arlington, Virginia.

8. Mosher, F. R., Report from the Space Science and Engineering Center, University of Wisconsin, 1974.

9. Raschke, E., VonderHaar, R., Pasternak, M., and Bandeen, W, NASA Technical Note TN D-7249, 1971.

10. Ruff, I., Koffler, R., Fritz, S., Winston, J.S., and Rao, P.K. NOAA Technical Report NESC-38, 1967

11. Shenk, W.E., and Solomonson, V.V., Journal of Physical Oceanography, Volume 2, pp. 157, 1972.

12. Sikula, G.J. and VonderHaar, T.H., Atmospheric Science Paper No. 185 from the Department of Atmospheric Science, Colorado State University, Ft. Collins, Colorado, 1972.